ELSEVIER

Journal of Nuclear Materials 278 (2000) 30–36

journal of nuclear materials

www.elsevier.nl/locate/jnucmat

AFM study of the surface deformation of austenitic stainless steel irradiated by He^+ ions

L. Liu[a], T. Mitamura[a], M. Niibe[b], H. Tsubakino[a], M. Terasawa[a,*]

[a] *Faculty of Engineering, Himeji Institute of Technology, Shosha 2167, Himeji 671-2201, Hyogo, Japan*

[b] *Laboratory of Advanced Science and Technology for Industry, Himeji Institute of Technology, Shosha 2167, Himeji 671-2201, Hyogo, Japan*

Received 25 September 1998; accepted 2 September 1999

Abstract

Atomic force microscopy (AFM) was employed to confirm the validity for studying the surface deformation by radiation damage. Distinct swelling was noted by AFM observation in austenitic stainless steel SUS316 specimens which were irradiated by 200 keV He^+ ions in the range of dose from 2.4×10^{16} He/cm^2 (0.6 dpa) to 7×10^{17} He/cm^2 (17.5 dpa) at 673, 773, 823 and 873 K. The step height due to He ion-induced swelling showed an obvious dependence on irradiation dose and temperature. It was found for the first time that sharp ridging along the grain boundaries occurred, suggesting He atom agglomeration at high doses and temperatures. © 2000 Elsevier Science B.V. All rights reserved.

PACS: 61.16.Ch; 61.72; 61.72M; 61.80

1. Introduction

Helium embrittlement caused by 14 MeV neutron irradiation is one of the key phenomena to control the lifetime of the first wall structures in fusion reactors [1]. In nuclear materials, nuclear transmutation produces helium atoms owing to (n, α) reaction. Consequently, at high temperature, these helium atoms agglomerate into bubbles that cause embrittlement of metallic materials. Even a level of ppm helium is deleterious to the materials. On the other hand, void swelling is one of the most serious radiation effects we have encountered in the history of nuclear reactor development. The swelling is evident at medium temperature at which fuel cladding in a fast breeder reactor (FBR) and also the first wall of a fusion reactor are designed to be used. Although some pure materials show significant voidage even at low dose, usual commercial alloys such as austenitic stainless steels show observable swelling at a dose higher than 10^{22} n/cm^2. The void formation is affected by (n, α)-produced helium. At high temperatures and high irradiation doses, the swelling caused by a large number of helium bubbles becomes significant [2].

A calibrated profilometer was used to investigate the influence of various solute elements on the swelling behavior by Gessel and Rowcliffe [3]. In their experiments, the step height of swelling due to Ni ion irradiation on the surface of the Fe–Cr–Ni alloy was detected at temperatures from 500°C (773 K) to 730°C (1003 K). The results showed that the step height corresponding to the void swelling became great with an increase in temperature. The step height had a maximum value when temperature was around 650°C (923 K) and then it decreased gradually when the temperature increased even higher.

Fenske et al. [4] have employed transmission electron microscopy (TEM) to find the effect of total dose on the depth distribution of cavities (voids or bubbles) in nickel irradiated with 500 keV $^4He^+$ at 500°C (773 K). They reported that He bubbles were created by He ion irradiation at high temperature and have a density peak around the end of the range.

* Corresponding author. Tel.: +81-792 67 4924; fax: +81-792 66 8868.

E-mail address: terasawa@esci.eng.himeji-tech.ac.jp (M. Terasawa).

PII: S 0 0 2 2 - 3 1 1 5 (9 9) 0 0 2 3 2 - 9

Atomic force microscopy (AFM) is a powerful technique developed recently for nano-scale observation of surface. AFM measurement has an outstanding feature of a non-destructive observation. The use of AFM to study the surface of irradiated materials may provide some new information concerning the irradiation damage of the surface on the nanometer scale. Radiation damage on the surface in the early stages is too difficult to be detected by ordinary techniques such as SEM. AFM is a candidate of effective methods for the observation of the early stage process of the radiation damage evolution. However, few AFM studies on observing the swelling introduced by ion irradiation on the stainless steels surface have so far been carried out.

In the present work, we try to apply AFM method to estimate the possibility of measuring the surface swelling. We present the experimental results of the surface swelling of SUS316 irradiated by He ions and the dependence of the surface swelling on irradiation dose and temperature using AFM technique. It is observed that a ridge appears along the grain boundary above certain temperature and dose. From the observed ridge in grain boundaries, we try to find and explain the critical conditions for the appearance of ridge, including irradiation temperature and dose.

2. Experiments

2.1. Specimens

The material used in the present work is commercial austenitic stainless steel SUS316 0.25 mm thick. The chemical compositions (wt%) are listed in Table 1. Specimens were cut by a laser cutting machine into rectangular pieces with the size of 10×15 mm^2. The specimens were mechanically polished first with 1000 and 1500 grit SiC paper, then with 3 and 1 μm Al_2O_3 powders and finally with 0.5 μm diamond paste for 100 h. Roughness measurements were performed on each polished specimen by means of AFM. The average surface roughness was suppressed to less than 10 nm rms. After mechanical polish, all the specimens were annealed in 1×10^{-5} Pa vacuum at 1323 K for 1 h, followed by water quenching.

2.2. Ion irradiation

200 keV He^+ ions were used for bombardment of the specimens in vacuum using a Cockcroft–Walton type accelerator (with 200 kV maximum terminal voltage) at Himeji Institute of Technology. The target chamber was evacuated to 1.1×10^{-5} Pa by a diffusion pump with liquid nitrogen trap. The ion beam was focused on the target through an aperture with a diameter of 12 mm so as to distribute uniformly all over the target surface. The number of displacements per atom (dpa) created in the peak damage region was calculated using the TRIM-95 computer code adopting the displacement energy of 40 eV. The ion beam was controlled to a displacement rate of about 3.1×10^{-4} dpa/s (1.2×10^{13} He/cm^2/s). Target temperature was varied between 673 and 873 K and the irradiation dose up to 7×10^{17} He/cm^2. During ion irradiation, the specimens were covered with a sheet of nickel mesh, which had square holes with a size of 70×70 μm^2 (250 mesh), in order to compare the effects of irradiated and unirradiated regions. Soon after the irradiation, the specimens were cooled in vacuum to room temperature.

2.3. The atomic force microscopy

The atomic force microscopy (AFM) measurement was performed in air at room temperature using a Nanoscope III an AFM equipment made by Digital Instruments. A piezo head with standard Si_3N_4 cantilever was mounted to the AFM instrument. The maximum scanning region of the head was 125×125 μm^2. The AFM image was acquired using the constant force

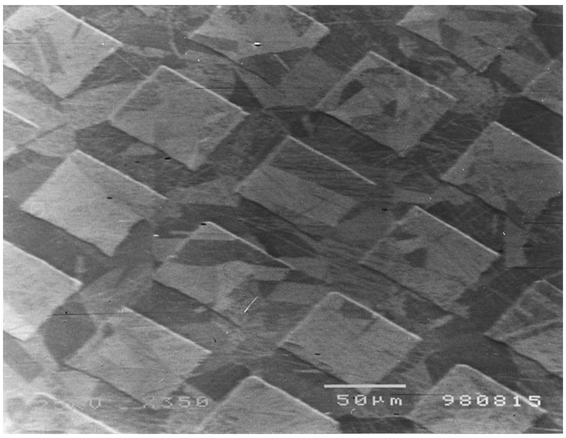

Fig. 1. Scanning electron micrograph of SUS316 surface masked with mesh after 200 keV He^+ ion irradiation at 873 K to a dose of 3×10^{17} He/cm^2 (7.5 dpa).

Table 1
Chemical composition (wt%) of the SUS316 alloy used in the present work

Fe	Cr	Ni	Mo	Mn	Si	P	C	S
Balance	16.79	10.30	2.16	1.17	0.68	0.027	0.06	0.001

mode on the tapping area. There was no frictional force between the piezo head and specimen surface in the tapping mode with a resolution less than 1 nm. The measurements of the surface step, which is the difference in level between the bombarded region and the unirradiated (masked) region, and unevenness of the irradiated surface were carried out. The scanning electron microscope (SEM) observation was also performed for a wide range inspection of the specimen surface.

3. Results and discussion

3.1. SEM image

Fig. 1 shows an example of SEM image of the surface of SUS316 irradiated by 200 keV He^+ ions up to a dose of 3×10^{17} He/cm^2 (7.5 dpa) at 873 K. Mesh-masked pattern is clearly observed, i.e., unirradiated region with a width of about 30 μm and irradiated area with 70 μm width. The appearance of this mesh pattern is evidence of radiation effects since the surface swelling, which will be discussed later, was induced in the irradiated region and deformation of the surface results in the change of the SEM image. Some grain patterns are observed with different contrast on the irradiated region.

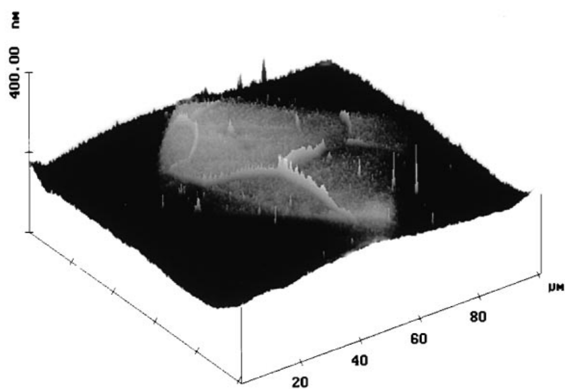

Fig. 2. A typical three-dimensional AFM image with a size of 100×100 μm^2 for SUS316 irradiated by 200 keV He^+ ions up to 1.5×10^{17} He/cm^2 (3.75 dpa) at 873 K.

3.2. The step height

Fig. 2 shows a typical AFM image of the SUS316 surface irradiated by He^+ ions with 1.5×10^{17} He/cm^2 (3.75 dpa) at 873 K. The upward expansion of the He ion-irradiated region can be observed with brighter image. The height of the expansion on the specimen, which is called henceforth as step height, is illustrated in Fig. 3. Fig. 3(a) shows a typical cross-sectional view selected from the surface image along the line shown in Fig. 3(b). In Fig. 3(a), the step height is about 100 nm, which is the average of the values obtained in ten randomly selected sections. The needle-like bump as shown in Fig. 3(a), which is called henceforth as a ridge, appears along a line corresponding to the grain boundary. This ridge can be seen in Fig. 2 as the brightest thin portions.

Three-dimensional AFM images of the specimens irradiated at 773 K with different dose levels are presented in Fig. 4(a)–(c). It is clearly seen from these AFM images that the step height depends directly on irradiation dose, indicating that surface swelling shown as the step height increases with increase in irradiation dose. The dose dependence of the step height is presented in Fig. 5. It can be roughly divided into two stages, slow increase in the irradiation dose below 3×10^{17} He/cm^2 and steep increase above 3×10^{17} He/cm^2. The slow increase is considered to correspond to the stage where

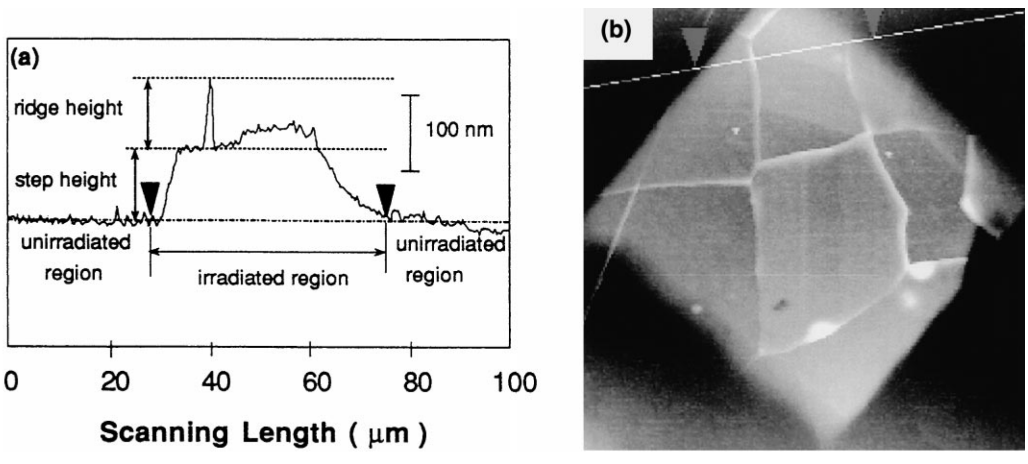

Fig. 3. A typical scheme of the step height and the ridge along grain boundaries in the 200 keV He ion-irradiated region (3×10^{17} He/cm^2, 873 K): (a) the cross-sectional view corresponding to the line indicated in (b).

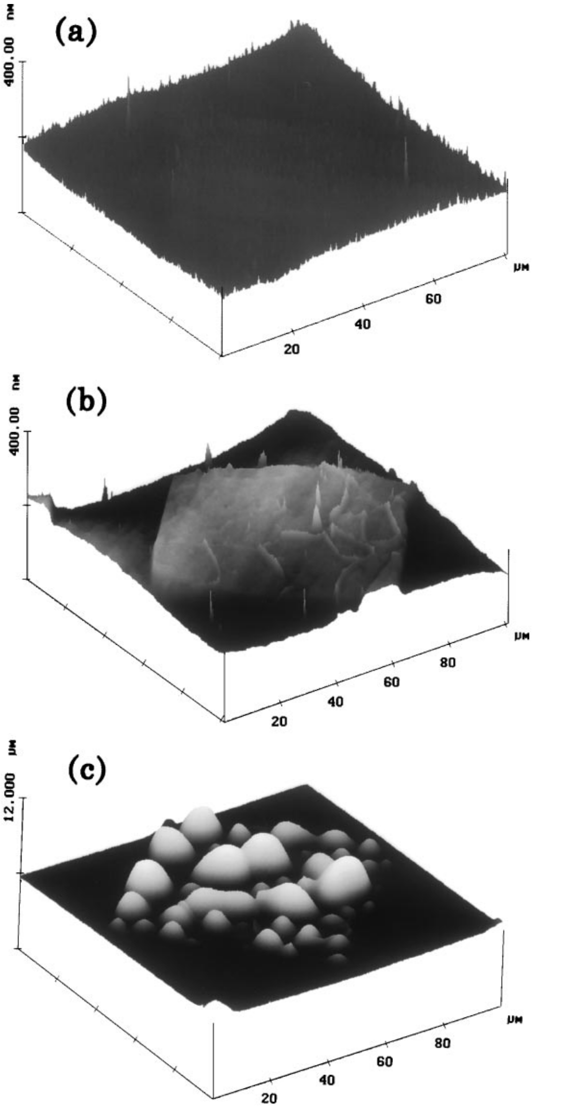

Fig. 4. AFM images of SUS316 irradiated by 200 keV He^+ ions at 773 K with different dose levels: (a) 7×10^{16} He/cm^2 (1.75 dpa), (b) 2×10^{17} He/cm^2 (5 dpa), and (c) 7×10^{17} He/cm^2 (17.5 dpa).

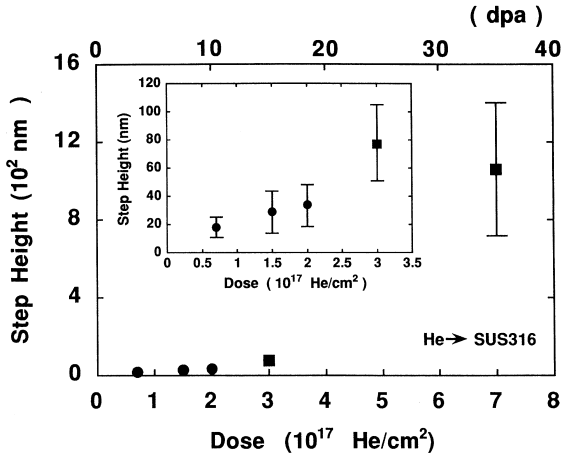

Fig. 5. A dose dependence of the step height for SUS316 irradiated by 200 keV He^+ ions at 773 K. The data are evaluated from the AFM images.

swelling is caused mainly by helium gas bubble accumulation, and the steep increase to the stage where the swelling is enhanced due to cavity growth through the interaction of the bubbles with irradiation-induced vacancies though we have not directly observed this process with AFM. Helium atoms are uniformly introduced as interstitial atoms into metals. They are trapped easily by vacancies produced by lattice atom displacement and agglomerate into small bubbles. In the present work, when the helium dose reaches 3.0×10^{17} He/cm^2, the step height begins to increase rapidly. It is suggested that at a critical number of helium atoms or a critical radius of helium bubbles, the bubbles agglomerate easily to bigger cavities and a qualitative change in growth kinetics of radiation damage takes place [5,7]. As a result, rapid increase of swelling appears. At 7.0×10^{17} He/cm^2, the step height reaches as high as 1000 nm. As shown in Fig. 4(c), many blisters with average diameter of about 30 µm are observed clearly. Some flakes are found in irradiated areas, though they are not shown in Fig. 4(c). It is suggested that bubble coalescence occurs in the surface layer and leads to increase of the integrated lateral stress in the surface area [4]. The stress becomes a driving force that leads to deformation of the surface layer. The inset in Fig. 5 shows the dose dependence of step height in low irradiation dose. It will be discussed later.

Fig. 6(a)–(d) show AFM images for the specimens irradiated with 3×10^{17} He/cm^2 at 673, 773, 823 and 873 K, respectively. An increase of the step height and ridge along grain boundaries with temperature is found. Fig. 7(a) and (b) illustrate the temperature and the dose dependence of the step height, respectively. In Fig. 7(a), there is no clear temperature dependence with 1.5×10^{17} He/cm^2 irradiation. In the case of the irradiation with 3×10^{17} He/cm^2, the step height increases with temperature. In Fig. 7(b), with the low irradiation dose, the approximately linear dependence of the step height on dose is shown at each temperature within the limit of error. This nearly linear relationship for the irradiation at 773 K has also been shown in the inset in Fig. 5. It is suggested that in low irradiation dose the increase of step height is proportional to the number of helium atoms. It is in agreement with the dose dependence of swelling volume fraction reported by Fenske for TEM observation [4]. They also reported that the radius and density of He bubbles increase with dose

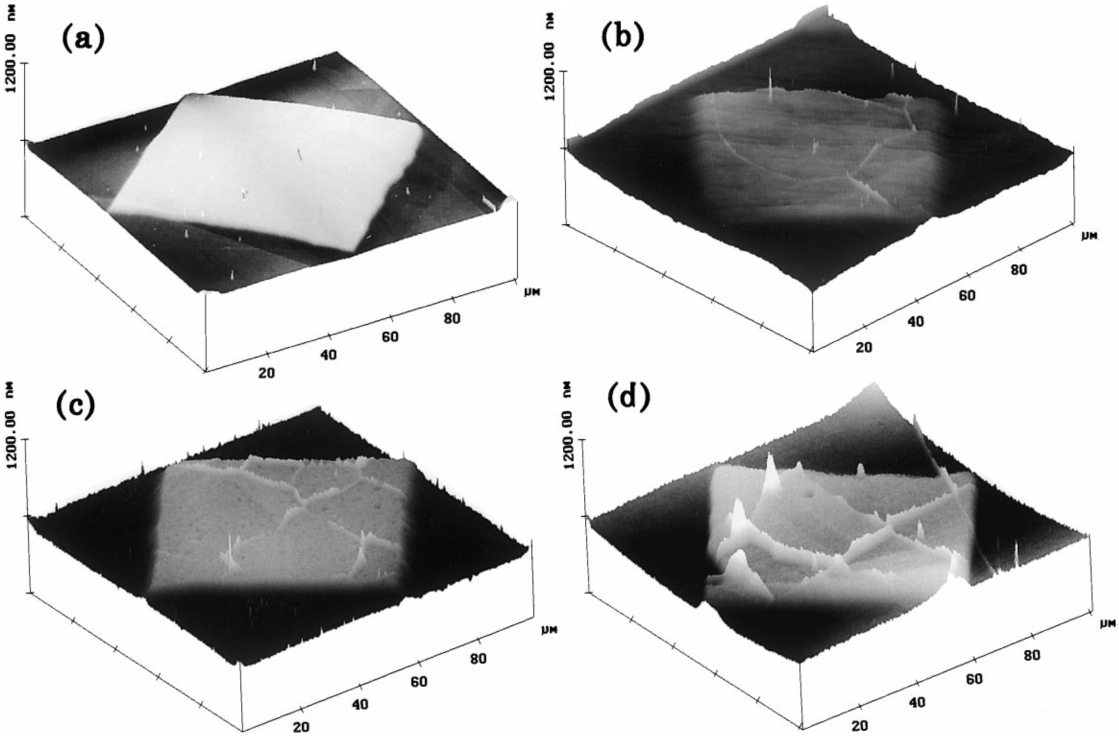

Fig. 6. AFM image of SUS316 irradiated by 200 keV He^+ ions with a dose of 3×10^{17} He/cm^2 (7.5 dpa) at the temperatures: (a) 673, (b) 773, (c) 823 and (d) 873 K.

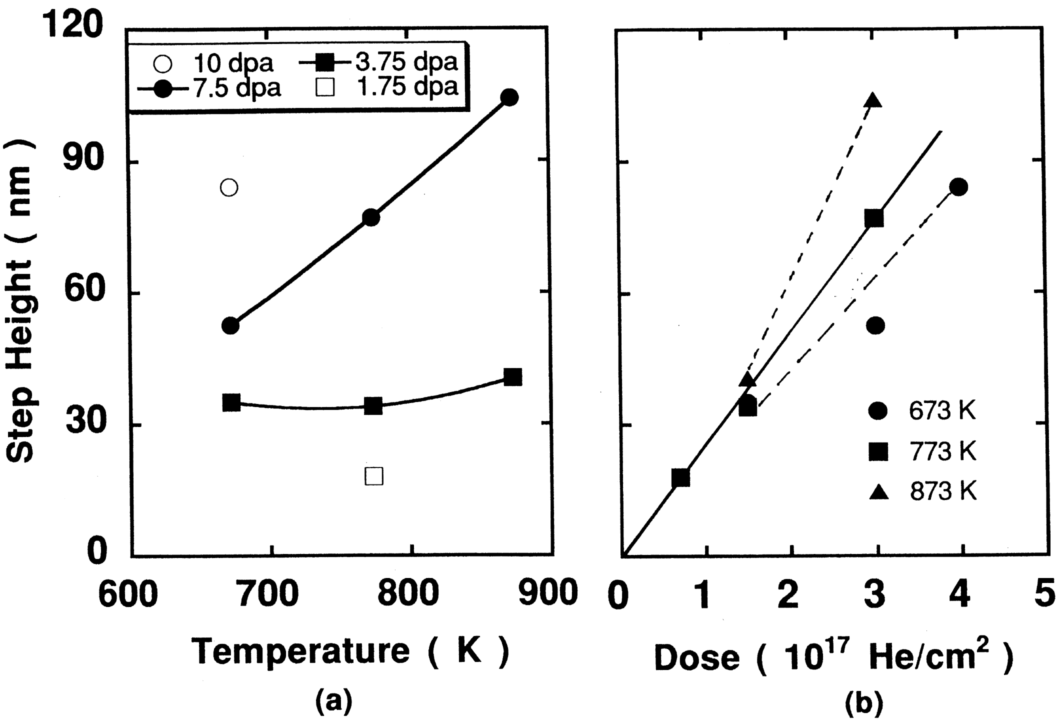

Fig. 7. A temperature dependence (a) and a dose dependence (b) of the step height for SUS316 irradiated by 200 keV He^+ ions with doses ranging from 7×10^{16} He/cm^2 (1.75 dpa) to 4×10^{17} He/cm^2 (10 dpa).

increase in low dose. The linear relationship of radiation effect vs. dose is shown in the irradiation-induced stress experiments by EerNisse and Picraux [6].

It is well known that the diameter of helium bubbles becomes bigger as the temperature increases, bubbles migrate easily at high temperatures to combine with each others becoming bigger bubbles, and, also, He atoms play a key role in void nucleation and growth. This may be the reason that swelling has a strong dependence on temperature at an irradiation dose of 3×10^{17} He/cm^2 and it is in agreement with the result in Refs. [1,3]. The step height is dependent not only on dose but also on temperature.

3.3. Ridge along grain boundaries

It is noted that a ridge appears on the irradiated grain boundaries under certain irradiation conditions. This ridge growth has not been reported so far. No ridge along grain boundaries can be observed with 7×10^{16} He/cm^2 (1.75 dpa) irradiation as shown in Fig. 4(a). However, as irradiation dose increases, the ridge along the grain boundaries becomes clear as shown in Fig. 4(b) and (c). The swelling along the grain boundary becomes more prominent, resulting in the increase of the ridge height. The ridge height is also dependent on the temperature, as suggested in Fig. 6(b)–(d)). In the case of 673 K, the ridge along the grain boundaries cannot be observed. While the temperature increases from 773 to 873 K, the ridge height along grain boundaries becomes higher.

Fig. 8 shows a dose–temperature relation to illustrate an appearance of the ridge along grain boundaries (solid circle: the ridge is observed, solid triangle: the ridge is not observed). It is suggested that there exists a critical condition for the appearance of the ridge. In the figure, a

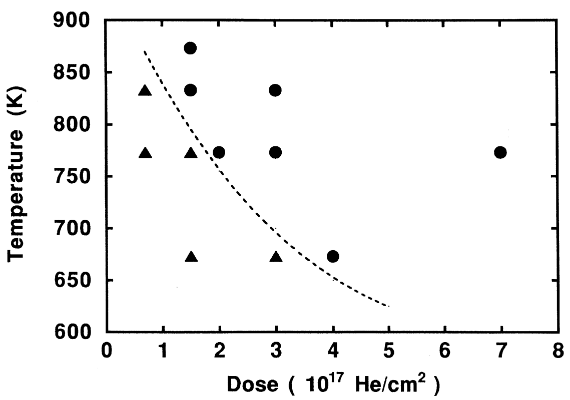

Fig. 8. Dose–temperature relation concerning the ridge formation. A speculated critical boundary line between the ridge formed and not formed region (solid circle: ridge is observed, solid triangle: ridge is not observed).

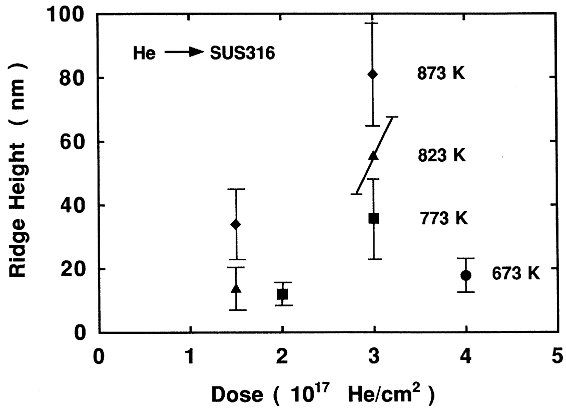

Fig. 9. A dependence of the ridge height along grain boundaries on He^+ ion irradiation doses.

tentative boundary line is shown for judgment on whether the ridge grows or not in a certain irradiation condition. Above this line, the ridge along the grain boundaries grows, which is observed to be more prominent in higher doses and higher temperatures. Below the line, the ridge is hardly observed. The key for understanding the irradiation effects on mechanical properties at high temperatures is a microstructure change [8–10]. The critical line in Fig. 8 will give a standard to judge the periphery of the region where He ion irradiation introduces such a structural change to the target materials. It is suggested that above the critical line, helium atoms easily migrate through the material, especially to the grain boundary. During this migrating process, the formation of helium bubbles and vacancy clusters takes place and helium bubbles grow rapidly to larger cavities at grain boundary. At low temperature and low dose, which is corresponding to the region below the critical line, no effective nucleation of helium bubbles or large cavities occurs and the ridge along the grain boundaries does not grow. Experimental determination of the critical line (or curve) may also be useful to estimate whether helium embrittlement occurs or not, in a certain irradiation condition.

The ridge heights evaluated at each temperature are shown in Fig. 9 as a function of dose. For each irradiation temperature, the ridge height increases with increase of irradiation dose. The growth rate at 873 K is slightly higher than that at 823 and 773 K.

4. Conclusions

Atomic force microscopy (AFM) has been successfully applied to study the surface deformation caused by radiation effects. For the austenitic stainless steel SUS316, bombarded with He ion under different irradiation conditions of irradiation dose and temperature, the non-destructive AFM observation revealed the surface deformation caused by radiation effects. A strong dependence of the step height in the irradiated region on irradiation conditions has been found. The step height increases sharply at high temperatures and high doses. In addition, it is found for the first time that the ridge appears along the grain boundary. This is one of the useful features of the non-destructive and nano-scale observation by AFM. The ridge height depends not only on irradiation dose but also on ambient temperature, suggesting that there exist critical dose and temperature for the ridge formation.

Acknowledgements

This work was supported by the Sasakawa Scientific Research Grant from The Japan Science Society. The authors are grateful to Dr T. Sekioka, Dr A. Yamamoto, and Dr S. Fukomoto for their valuable and kind help.

References

[1] M. Terasawa, M. Shimada, T. Kakuma, T. Yokitoshi, K. Shiraishi, K. Uematsu, in: M.L. Bleiberg, J.W. Bennett (Eds.), Radiation Effects in Breeder Reactor Structural Materials, Plenum, New York, 1977, p. 687.

[2] M. Terasawa, K. Fukushima, S. Nakahigashi, K. Ebisawa, M. Iimura, Jpn. J. Appl. Phys. 25 (1986) 1106.

[3] G.R. Gessel, A.F. Rowcliffe, in: M.L. Bleiberg, J.W. Bennett (Eds.), Radiation Effects in Breeder Reactor Structural Materials, Plenum, New York, 1977, p. 431.

[4] G. Fenske, S.K. Das, M. Kaminsky, G.H. Miley, J. Nucl. Mater. 85&86 (1979) 707.

[5] L.K. Mansur, J. Nucl. Mater. 216 (1994) 97.

[6] E.P. EerNisse, S.T. Picraux, J. Appl. Phys. 48 (1977) 9.

[7] E.H. Lee, L.K. Mansur, Philos. Mag. A. 52 (1985) 493.

[8] P.B. Johnson, P.W. Gilbert, Nucl. Instrum. and Meth. B 127&128 (1997) 734.

[9] F. Bates, W.G. Johnston, in: M.L. Bleiberg, J.W. Bennett (Eds.), Radiation Effects in Breeder Reactor Structural Materials, Plenum, New York, 1977, p. 625.

[10] S. Herbert, J. Nucl. Mater. 155–157 (1988) 1032.